Journal of Wind Engineering & Industrial Aerodynamics 167 (2017) 41–50

Contents lists available at ScienceDirect

Journal of Wind Engineering and Industrial Aerodynamics

journal homepage: www.elsevier.com/locate/jweia

# Wind tunnel study of wind-induced torques on L-shaped tall buildings

Yi Li[a,b], Q.S. Li[c,*], Fubin Chen[d]

[a] School of Civil Engineering, Hunan University of Science and Technology, Xiangtan 411201, Hunan, China
[b] Hubei Key Laboratory of Roadway Bridge and Structure Engineering, Wuhan University of Technology, Wuhan 430070, Hubei, China
[c] Department of Architecture and Civil Engineering, City University of Hong Kong, Kowloon, Hong Kong, China
[d] School of Civil Engineering and Architecture, Changsha University of Science & Technology, Changsha, Hunan, China

ARTICLE INFO

*Keywords:*
Tall buildings
Wind tunnel test
Wind-induced torque

ABSTRACT

L-shaped tall buildings are commonly built in urban areas due to shortage of land and graceful demand of architectural design. In this study, eight L-shaped rigid models with different geometric dimensions are tested in a boundary wind tunnel to study the characteristics of the wind-induced torques acting on L-shaped tall buildings. RMS force coefficients, power spectral densities and vertical correlation functions of the wind-induced torques are analyzed and discussed in details. Based on the wind tunnel test results, empirical formulas which take the buildings' side ratio and terrain category as key variables are proposed for estimating the wind-induced torques on L-shaped tall buildings. A simplified expression to evaluate the wind-induced torques on L-shaped tall buildings is derived based on the proposed formulas and its applicability has been verified by a case study. This study aims to provide a simple and effective way for the estimation of wind induced torque on L-shaped tall buildings.

## 1. Introduction

A large number of irregular shaped tall buildings have been built in recent years due to shortage of land in urban areas and graceful demand of architectural design. The irregular shapes of these buildings may make them more sensitive to wind excitations than regular shaped tall buildings, especially in across-wind direction and torsional moments. It has been widely recognized that external shapes of tall buildings play an important role in the generation of wind loads on high-rise structures. However, current design codes and standards (AIJ, 2004; ASCE, 2010; GB50009, 2012) generally only provide guidelines for estimating the wind effects on tall buildings with regular and symmetric shapes. Actually, there is no analytical formula available for evaluation of the wind effects on irregular shaped tall buildings. Therefore, it is necessary to conduct extensive research works on this topic.

Stathopoulos and Zhou (1993) adopted numerical simulation methods to predict the wind pressures on surfaces of various buildings with sharp corners. Gomes et al. (2005) investigated the wind effects on L and U-shaped building models by use of both wind tunnel testing and numerical simulation approach. Gu (2009) carried out wind tunnel tests on 27 typical tall building models and analyzed the characteristics of wind-induced pressures and forces on these buildings. Cluni et al. (2011) compared the wind loads on regular and irregular tall buildings by high order moment statistical analysis. Kim and Kanda (2013) investigated the spatial-temporal characteristics of pressure fluctuations on tapered and set-back tall buildings. Chakraborty et al. (2014) investigated the wind pressure distributions on a '+' shaped tall building by wind tunnel testing and numerical simulation. Cheng et al. (2015) studied the characteristics of fluctuating wind pressures on side faces of H-shaped tall buildings and the shape effect on the generation of across-wind forces with the space-time statistical tool of proper orthogonal decomposition.

The previous studies on the wind effects on irregular shaped tall buildings mostly focused on the pressure distributions on tall building models but rarely referred to the overall wind loads especially torsional loads. It has been reported that wind induced displacements and accelerations at corners of tall buildings can be amplified by the wind-induced torsional vibration and cause uncomfortable feeling of the residents (Tallin and Ellingwood, 1984, 1985). Liang et al. (2004) studied the torsional wind loads on rectangular tall buildings and established empirical formulas of base torque spectra. Li et al. (2014) investigated the characteristics of wind-induced torques on rectangular tall buildings and presented a simplified expression to evaluate the dynamic torsional wind loads. It is well known that the mechanisms of generation of wind-induced torques, such as the wake excitation, are strongly correlated with external shapes of tall buildings. However, the provisions stipulated in design codes and standards are established

* Corresponding author.
*E-mail address:* bcqsli@cityu.edu.hk (Q.S. Li).

http://dx.doi.org/10.1016/j.jweia.2017.04.013
Received 22 September 2016; Received in revised form 18 April 2017; Accepted 20 April 2017
0167-6105/

**Fig. 1.** Examples of L-shaped tall buildings.

mainly from experimental results of regular building models like square or rectangular sectional models. Hence, estimation of wind-induced torques on irregular shaped tall buildings based on current provisions may not be reasonable. In recent years, a large number of L-shaped tall buildings have been built throughout the world. Fig. 1 shows examples of L-shaped buildings. The overall wind loads acting on L-shaped tall buildings including along-wind and across-wind forces as well as and torques have rarely been reported. Based on extensive wind tunnel tests, the along-wind and across-wind loads on L-shaped tall buildings have been studied in detail and related spectra and parameters for evaluating these wind loads have been proposed (Li, 2014; Li and Li, 2016). However, there is lack of guideline for estimation of the wind-induced torques on complex structures with torsional irregularity such as L-shaped tall buildings.

In this paper, eight L-shaped tall building models with different geometric dimensions are tested by simultaneous pressure measurement technique in a boundary wind tunnel to study the characteristics of wind-induced torques acting on L-shaped tall buildings. Based on the experimental results, RMS force coefficients, power spectral densities and vertical correlation functions of the wind-induced torques are presented and discussed, and empirical formulas are proposed by use of the none linear least-squares method (NLSM). In the light of structural dynamics method and random vibration theory, a simplified expression to evaluate the wind-induced torques on L-shaped tall buildings is derived based on the proposed formulas. The applicability of the proposed simplified formula is verified through a case study.

## 2. Wind tunnel test

Due to complex mechanisms of generation of torques on bluff bodies, it is difficult to deduce analytical formulas for estimation of wind induced torque on tall buildings. It has been widely accepted that wind tunnel test is the most effective tool to study the characteristics of wind-induced torques on tall buildings.

### 2.1. Features of approaching wind flows

Wind tunnel test was conducted in a boundary layer wind tunnel laboratory at Hunan University, China. In order to evaluate the effects of terrain category, four different kinds of terrain categories specified in the Loads Standard Code of China (GB50009-2012) were simulated by different combinations of spires and roughness elements in the wind tunnel test. Due to limited space of this paper, only the profiles of mean wind speed and turbulence intensity of terrain category C at a length scale 1:500 are illustrated in Fig. 2, while the profiles and related information of the other wind fields simulated in the wind tunnel test

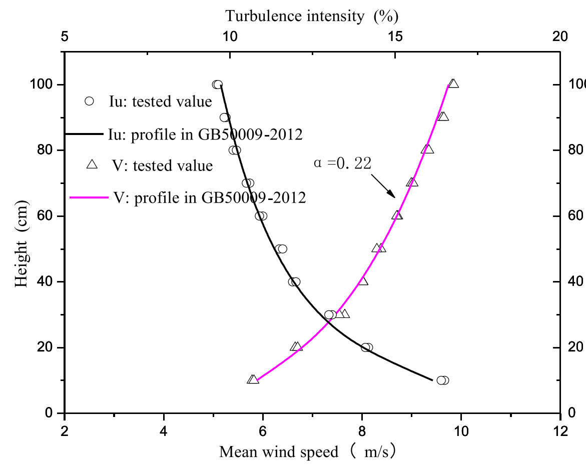


**Fig. 2.** Mean wind speed and turbulence intensity profiles in category C.

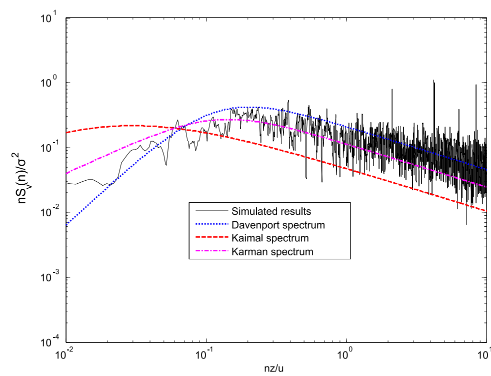


**Fig. 3.** Longitudinal velocity spectra at reference height of 0.6 m.

were described in Li (2014). The corresponding longitudinal velocity spectra of the simulated boundary layer flows at the reference height of 0.6 m above the floor of the wind tunnel test section are plotted in Fig. 3, which are in good agreement with the von Karman spectrum. In addition, the experiments were also conducted in uniform smooth flow for comparison purposes.

### 2.2. Test arrangements

Eight rigid models with different configurations of L-shape (called M1, M2, M3, M4, M5, M6, M7, M8) were built for the wind tunnel test and their geometric parameters are shown in Table 1. It can be seen that M1, M2, M3, M5, M7, M8 are L-shaped models with different side ratios D/B, while M4, M5, M6 are those with different aspect ratios H/B. All the test models were made of ABS (Acrylonitrile Butadiene Styrene) material to ensure sufficient strength and rigidity of the models. Pressure taps on the models were connected to electronic pressure scanning modules by plastic tubes. Numerical compensation was employed to correct the tubing effects prior to data processing (Li, 2014). The maximum blockage ratio in the wind tunnel experiment was about 1.3% for all the models tested in this study.

Fig. 4 shows the definition of wind direction and locations of pressure taps on the experimental models. The mean wind speed at the gradient height was kept as 12 m/s for the wind tunnel test of all the models. Electronic pressure scanning modules made by Scanivalve Inc. (USA) were used to measure instantaneous wind-induced pressures on the surfaces of the models. Pressure measurements on the L-shaped models were conducted for wind direction from 0° to 360° at 10° intervals with additional directions 45°, 135°, 225°, 315° so that the total number of wind direction considered in the model test was 40. The data sampling frequency was set to be 312.5 Hz and the sampling

**Table 1**
Geometric parameters of the test models.

| Models | Height H (mm) | Breadth B (mm) | Depth D (mm) | Thickness d (mm) | Side ratio D/B | Aspect ratio H/B | Pressure taps |
|---|---|---|---|---|---|---|---|
| M1 | 500 | 100 | 50 | 40 | 0.5 | 5.0 | 250 |
| M2 | 500 | 100 | 80 | 40 | 0.8 | 5.0 | 310 |
| M3 | 500 | 100 | 100 | 40 | 1 | 5.0 | 320 |
| M4 | 400 | 100 | 120 | 40 | 1.2 | 4.0 | 228 |
| M5 | 500 | 100 | 120 | 40 | 1.2 | 5.0 | 360 |
| M6 | 600 | 100 | 120 | 40 | 1.2 | 6.0 | 432 |
| M7 | 500 | 100 | 150 | 40 | 1.5 | 5.0 | 400 |
| M8 | 500 | 100 | 200 | 40 | 2.0 | 5.0 | 440 |

length was 32 s. The total number of the data obtained from a pressure tap was 10, 000 for each wind direction.

## 3. Results and discussions

Time series of wind-induced torque at each measurement layer on an L-shaped model can be obtained by integrating the simultaneously measured wind pressures on that layer. Mean and RMS torque coefficients are defined as

$$C_T(z_i) = \frac{\overline{F_T}(z_i)}{A(z_i)Dq_H} \quad C_T'(z_i) = \frac{\sigma_{F_T}(z_i)}{A(z_i)Dq_H} \tag{1}$$

$$C_{M_T} = \frac{\overline{M_T}}{BDHq_H} \qquad C_{M_T}' = \frac{\sigma_{M_T}}{BDHq_H} \tag{2}$$

where, $C_T(z_i)$ and $C_T'(z_i)$ are mean and RMS torque coefficients; $\overline{F_T}(z_i)$ and $\sigma_{F_T}(z_i)$ are mean and RMS torque at height of $z_i$; $C_{M_T}$ and $C_{M_T}'$ are mean and RMS base torsional moment coefficients; $\overline{M_T}$ and $\sigma_{M_T}$ are mean and RMS base torsional moments. $A(z_i)$ is the frontal area of each measurement layer; $H$ is the height of a model; $B$ is the breadth in the direction perpendicular to the wind and $D$ is the model depth in the direction parallel to the wind; $q_H = 0.5\rho U_H^2$ stands for the reference wind dynamic pressure, $\rho$ is the air mass density, generally is 1.25 $kg/m^3$,$U_H$ is mean wind speed at the top of a model.

### 3.1. Torque coefficients

#### 3.1.1. Effects of terrain category

The effects of terrain category on torque coefficients are similar for all the L-shaped models. Hence, the torque coefficients of the fourth layer on model M3 are selected to discuss the effects of the terrain category on the wind induced torque of L-shaped tall buildings. Fig. 5 shows the variations of the mean and RMS torque coefficients of model M3 with wind direction under different terrain conditions. The terrain category has little effect on the mean torque coefficients in all wind directions. There are two peaks appeared in the variations of the mean torque coefficients. But the magnitudes of the two peaks are not the same due to the asymmetry of the building shape. The corresponding wind directions of the two peaks are about 110° and 280°, respectively. The mean torque coefficients range from −0.25 to 0.25 under all wind directions. The RMS torque coefficients gradually increase as the terrain category changes from A to D (from smoother to rougher terrains). The results of terrain category D are obvious larger than those of the other terrains, indicating that the higher level of turbulence results in the increase of the dynamic wind induced torque. The RMS torque coefficients range from 0.02 to 0.08 in all wind directions. The maximum and minimum values of the RMS torque coefficients occur at wind direction of 90° and 45°, respectively. It should be pointed out that the wind directions corresponding to the peak values of the RMS torque coefficients are consistent with those of lift coefficients of L-shaped tall buildings (Li and Li, 2016), implying that strong correlation exists between the torque and lift coefficients. Tang (2006) identified that wind direction of 90° is generally the unfavorable direction for generation of the maximum wind induced torque on L-shaped tall buildings. The results of this study illustrate that both mean and RMS torque components reach their maximum values around wind direction of 90°. On the other hand, the Loads Standard Code of China (GB50009-2012) only requires considering the wind-induced torques on L-shaped buildings under wind direction of 90° in the wind-resistant design. Hence, wind direction of 90° was chosen as the unfavorable wind direction to discuss the effects of side ratio and aspect ratio on the mean and RMS torque coefficients of L-shaped buildings in the following parts of this paper.

#### 3.1.2. Effects of side ratio

Variations of mean and RMS torque coefficients with different side ratios are shown in Fig. 6. It can be observed that the mean torque coefficients range from 0.12 to 0.28, which is different from those of rectangular tall buildings (Lin et al., 2005). The mean torque coefficients gradually increase as the side ratio becomes larger. This is mainly caused by intensive eccentric loads on face ② and face ④ resulted from the increasing depth. The maximum value of mean torque coefficients arrive at 0.28 when the side ratio is 2.0. As the model height increases, the mean torque coefficients of all the L-shaped models firstly increase and then decrease, while the maximum value emerges at approximately 0.75$H$. The RMS torque coefficients change little as the height of the models increases but slightly increase as the side ratio becomes larger, and the maximum value is close to 0.10.

#### 3.1.3. Effects of aspect ratio

Fig. 7 presents the variations of mean and RMS torque coefficients with different aspect ratios. As the aspect ratio increases, the mean torque coefficients of M4 (H/B=4.0) are approximately the same with those of M5 (H/B=5.0) up to z/H=0.5. The mean torque coefficients of M6 (H/B=6.0) are larger than those of the other two models along the height of the models. The RMS torque coefficients change little as the aspect ratio increases. This illustrates that the effects of aspect ratio are insignificant, implying that it may not be necessarily taken into account in the estimation of the wind-induced torques on L-shaped tall buildings.

### 3.2. Base torsional moment coefficients

Variations of mean and RMS base torsional moment coefficients with wind direction for all the building cases are shown in Fig. 8. The mean and RMS base torsional moment coefficients vary with wind direction in consistent patterns with those of the torque coefficients. The mean base torsional moment coefficients range from −0.14 to 0.28 in all wind directions and are obviously larger than those of rectangular tall buildings (Tang, 2006). The RMS base torsional moment coefficients range from 0.009 to 0.065. The two peak values of the mean base torsional moment coefficients are close to each other when the side ratio of an L-shaped tall building is 1.0 due to its geometrical symmetry. As the side ratio increases, asymmetrical pressure distributions on face ② and face ④ result in increasing value of the first peak, while the second peak value changes little except for model M1. The

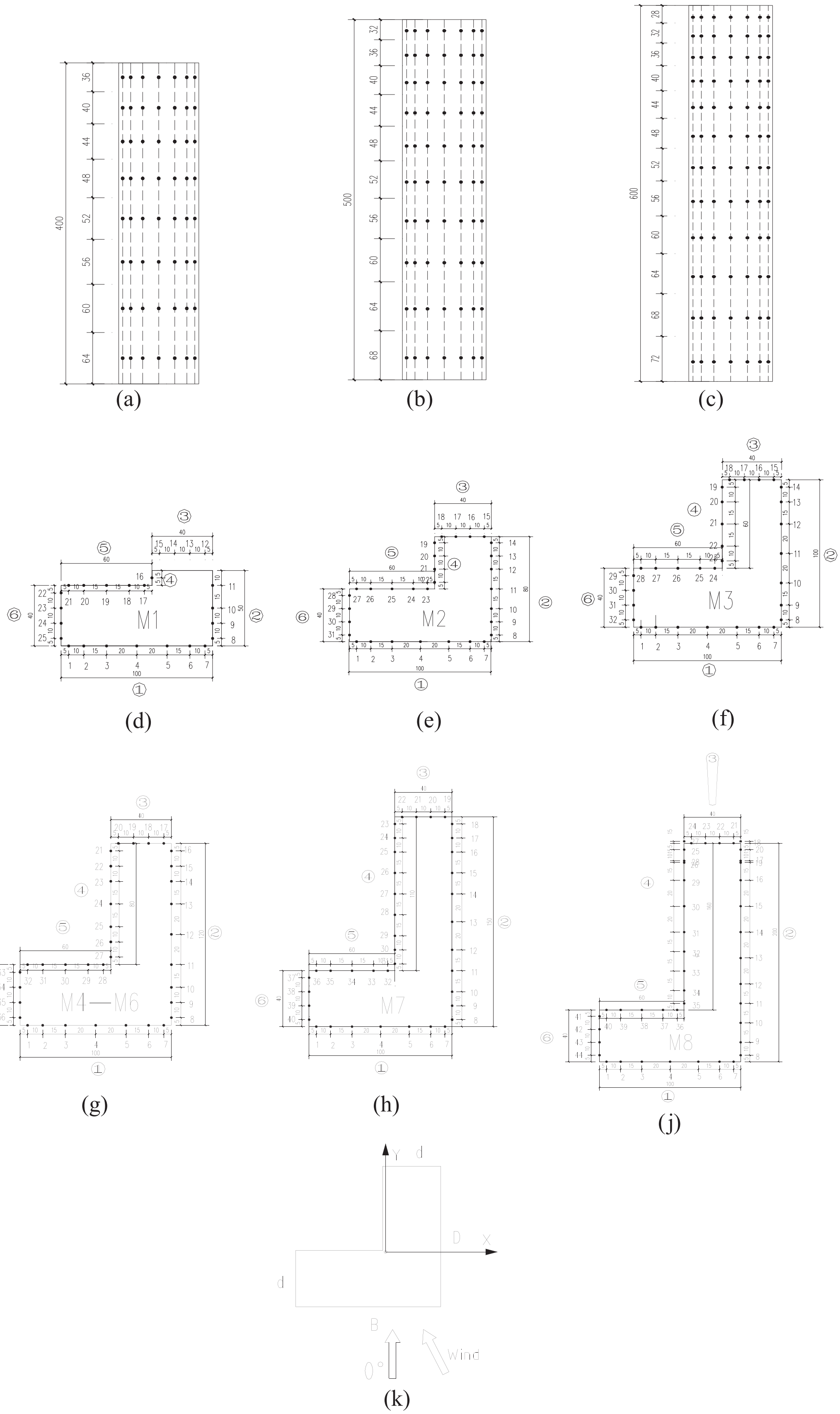


**Fig. 4.** Definition of wind direction and location of pressure taps: (a)–(c) measurement layers, (d)–(j) distributions of pressure taps, (k) definition of wind direction.

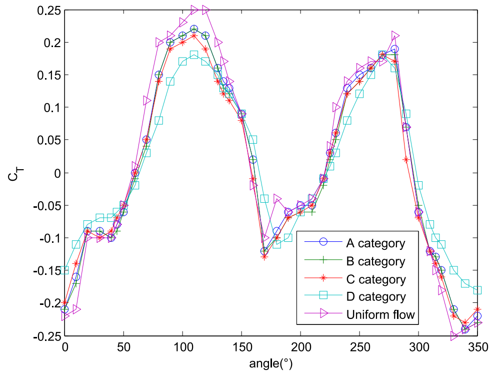


(a) Mean torque coefficients

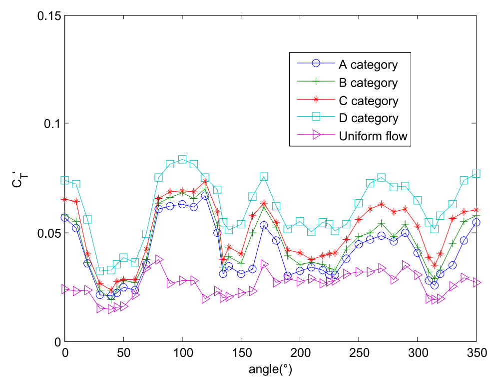


(b) RMS torque coefficients

**Fig. 5.** Variations of mean and RMS torque coefficients of model M3 with wind direction for different terrain categories.

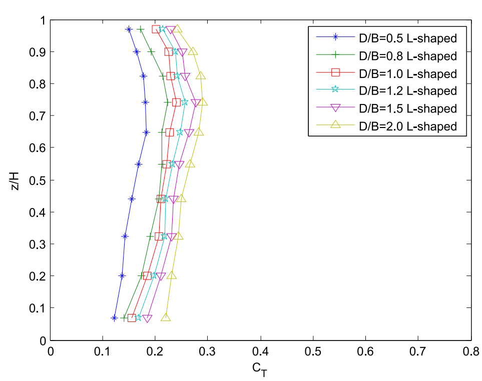


(a) Mean torque coefficients

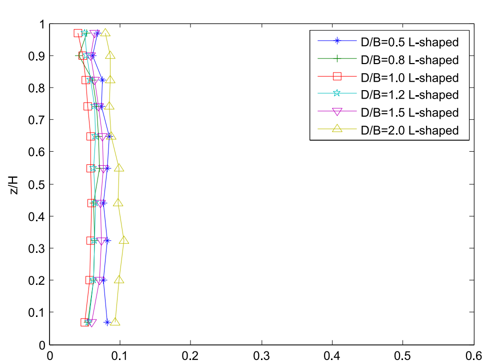


(b) RMS torque coefficients

**Fig. 6.** Variations of mean and RMS torque coefficients with side ratio.

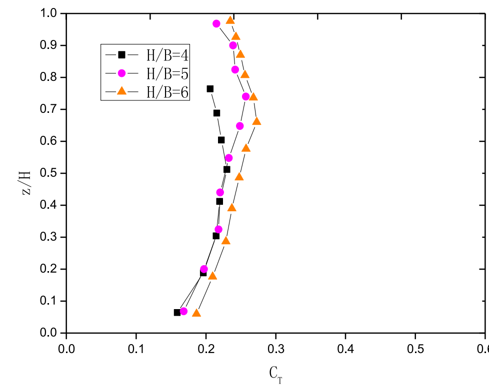


(a) Mean torque coefficients

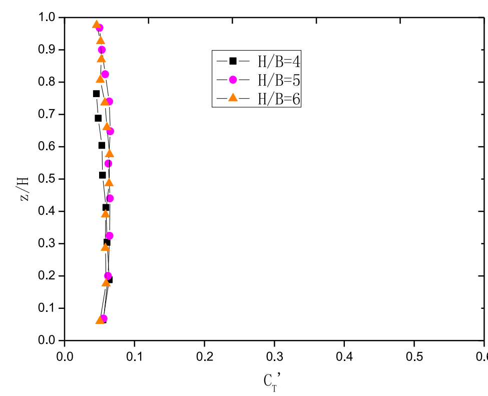


(b) RMS torque coefficients

**Fig. 7.** Variations of mean and RMS torque coefficients with aspect ratio.

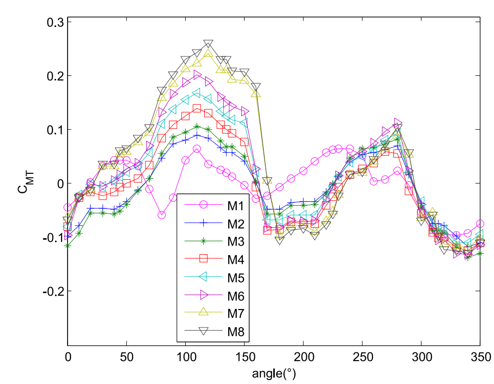


(a) Mean base torque coefficients

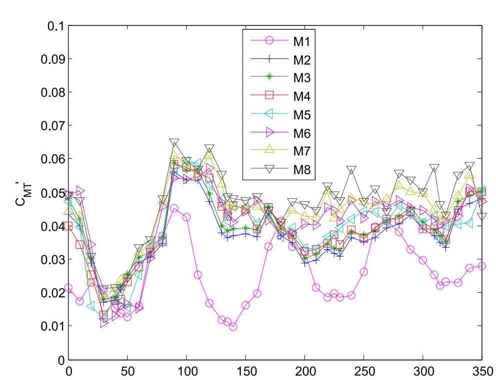


(b) RMS base torque coefficients

**Fig. 8.** Variations of mean and RMS base torque coefficients with wind direction.

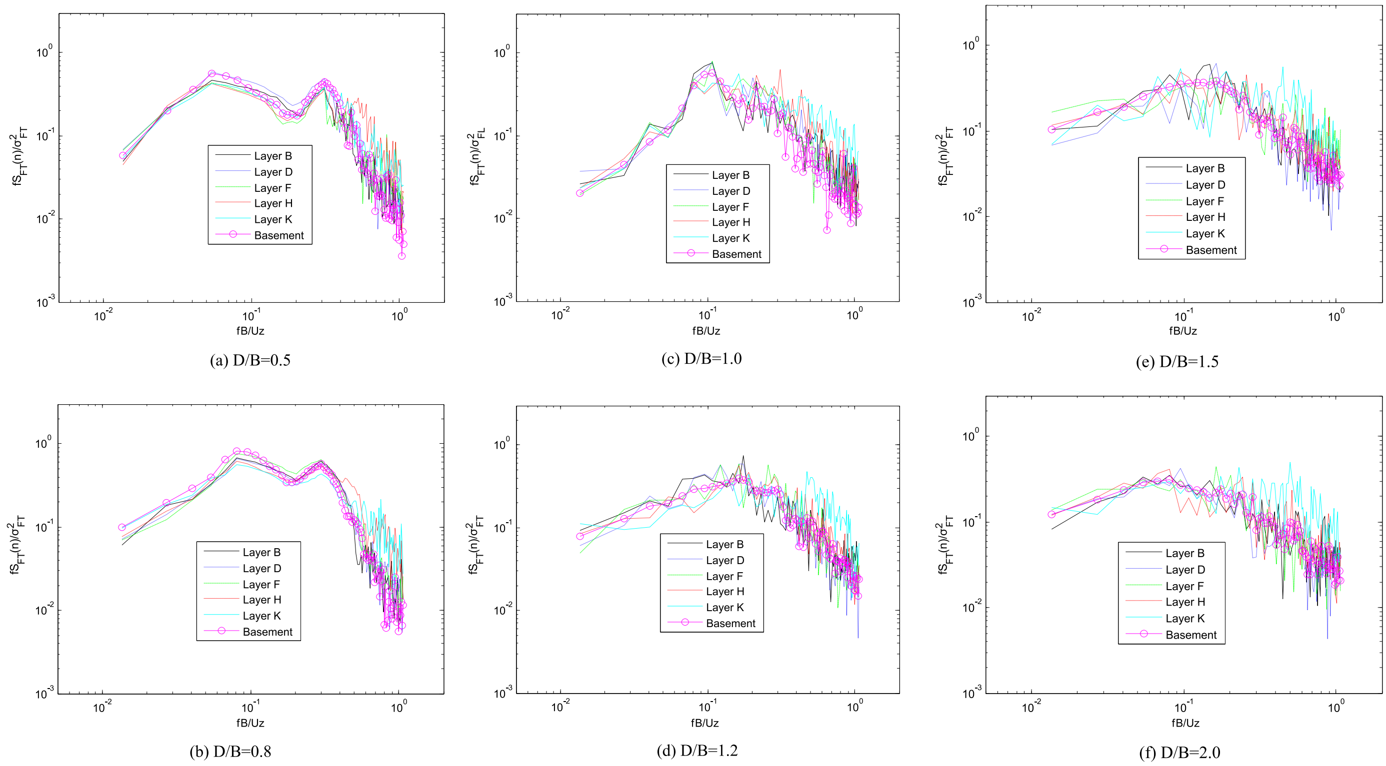


**Fig. 9.** Torque spectra of L-shaped building models with various geometric dimensions.

aspect ratio has no influence on the RMS base torsional moment coefficients.

### 3.3. Power spectral densities

The power spectral densities of wind-induced torques are obtained for all the L-shaped models. Fig. 9 presents the torque spectra of the L-shaped models with various geometric dimensions under the unfavorable wind direction of 90°. It can be observed from the figure that the variations of the spectra of the base torque with reduced frequency are almost the same as those of the torque spectra at each measurement layer on the models. When $D/B < 1$, there are two peaks emerged in the torque spectra, which are similar with those of rectangular tall buildings when the approaching flow is perpendicular to face ②. The two peaks are associated with the phenomena of vortex shedding and reattachment of separated flows on the side wall, respectively. When $D/B = 1$, due to vortex shedding from the models, there is only a narrow-band peak emerged in the torque spectra and the reduced frequencies corresponding to the single peak is close to the Strouhal number (0.1) of rectangular cylinders. As the side ratio $D/B$ continues to increases, the increasing area of the windward face makes the along-wind forces increase so that the torque spectra are becoming similar with the longitudinal velocity spectra.

### 3.4. Mathematical model of torsional dynamic loads on L-shaped tall buildings

According to the theory of random vibration, the cross power spectra density $S_F(z_i, z_j; f)$ of wind-induced torques on different heights can be calculated by the following expression:

$$S_F(z_i, z_j; f) = \sigma_F(z_i)\sigma_F(z_j)S_F'(f)Cor_F(z_i, z_j) \tag{3}$$

where $\sigma_F(z_i)$, $\sigma_F(z_j)$ are the RMS torque coefficients at heights of $z_i$ and $z_j$, respectively. $S_F'(f) = \frac{S_{MT}(f)}{\sigma_{MT}^2}$ stands for non-dimensional base torsional moment spectrum. $Cor_F(z_i, z_j)$ is vertical correlation coefficient of torque coefficients.

Non-dimensional base torsional moment spectrum, RMS torque coefficients and vertical correlation coefficients are three key factors to determine the cross-spectral density of the wind-induced torques in Eq. (3). Since it is difficult or even impossible to derive the analytical expression of Eq. (3), numerical computation based on wind tunnel test results is the common method to deal with this problem. The nonlinear least-squares method (NLSM) is adopted in this study to establish empirical formulas based on the experimental results of the wind tunnel test. The side ratio $\alpha_{DB}$ and terrain category $\alpha_{TR}$ are chosen as two key factors as follows

$$\alpha_{DB} = D/B \quad \alpha_{DB} \in [0.5,\ 2.0] \tag{4}$$

$$\alpha_{TR} = \begin{cases} 1, & Category\ \ A \\ 2, & Category\ \ B \\ 3, & Category\ \ C \\ 4, & Category\ \ D \end{cases} \tag{5}$$

#### 3.4.1. Power spectral density of base torsional moment

The following normalized formula of the base torsional moment spectra of L-shaped tall buildings is proposed through non-linear fitting of the wind tunnel testing results.

$$\frac{fS_{MT}(f)}{\sigma_{MT}^2} = \frac{af}{(1+bf^c)^d} + \sum_{j=1}^{N} \frac{K_j(f/F_j)^2}{[1-(f/F_j)^2]^2 + 4P_j^2(f/F_j)^2} \tag{6}$$

where, the first item $\frac{af}{(1+bf^c)^d}$ represents the contribution of turbulence from approaching flows; in the second item $\sum_{j=1}^{N} \frac{K_j(f/F_j)^2}{[1-(f/F_j)^2]^2 + 4P_j^2(f/F_j)^2}$ j=1 denotes the contribution of vortex shedding from face ①, while j=2 stands for the contribution of reattachment of separated flow on face ①. When the side ratio $D/B$ is smaller than 1.0, N is equal to 1. As the side ratio increases, N is equal to 2. Parameters $K_j$,$P_j$,$F_j$,$a$,$b$,$c$ and $d$ in Eq. (6) are functions of the side ratio $\alpha_{DB}$ and the terrain category $\alpha_{TR}$. These parameters were determined based on the wind tunnel test results as follows

$$a = -6.9823 + 0.3134\alpha_{TR} + (13.4515 + 0.6880\alpha_{TR})\alpha_{DB} - (3.4629 + 0.2505\alpha_{TR})\alpha_{DB}^{2} \tag{7}$$

$$b = 1/(0.0311 - 0.0060\alpha_{TR} + (0.0604 - 0.0126\alpha_{TR})\alpha_{DB} + (0.0236 - 0.0041\alpha_{TR})\alpha_{DB}^{-2}) \tag{8}$$

$$c = 5.4331 - 0.2057\alpha_{TR} + (0.6878 + 0.1688\alpha_{TR})\alpha_{DB} + (0.4512 + 0.2114\alpha_{TR})\ln(\alpha_{DB})\alpha_{DB}^{-2} \tag{9}$$

$$d = 2.1990 - 0.3324\alpha_{TR} + (6.3874 - 0.8647\alpha_{TR})\alpha_{DB}^{-0.5} + (4.8282 - 0.6095\alpha_{TR})\alpha_{DB}^{-1.5} + (4.9017 + 0.5906\alpha_{TR})\alpha_{DB}^{-2} \tag{10}$$

$$K_1 = 0.0443 - 0.0058\alpha_{TR} + (0.0337 - 0.0054\alpha_{TR})\alpha_{DB}^{2} + (0.0039 + 0.0044\alpha_{TR})e^{\alpha_{DB}} \tag{11}$$

$$P_1 = (0.5440 + 0.3261\alpha_{TR})e^{[-(0.3827+1.0889\alpha_{TR})\alpha_{DB}^{-1}-(0.2189+0.1982\alpha_{TR})\alpha_{DB}]} + 0.0225 + 0.0030\alpha_{TR} \tag{12}$$

$$F_1 = 0.1063 - 0.0213\alpha_{TR} - (0.0330 - 0.0069\alpha_{TR})\ln(\alpha_{DB})\alpha_{DB} - (0.0143 - 0.0324\alpha_{TR})\alpha_{DB}^{-2} \tag{13}$$

$$K_2 = 0.0395 - 0.1088\alpha_{TR} + (0.1145 - 0.1202\alpha_{TR})\alpha_{DB}^{2} + (0.0023 + 0.0052\alpha_{TR})e^{\alpha_{DB}} \tag{14}$$

$$P_2 = (0.4395 + 0.3158\alpha_{TR})e^{[-(0.3215+0.9658\alpha_{TR})\alpha_{DB}^{-1}-(0.2458+0.1459\alpha_{TR})\alpha_{DB}]} + 0.0273 + 0.0028\alpha_{TR} \tag{15}$$

$$F_2 = 0.1282 - 0.0358\alpha_{TR} - (0.2384 - 0.3275\alpha_{TR})\ln(\alpha_{DB})\alpha_{DB} - (0.3493 - 0.2635\alpha_{TR})\alpha_{DB}^{-2} \tag{16}$$

Comparisons of the base torsional moment spectra by the proposed formulas and the wind tunnel test results are shown in Fig. 10. It can be found that the base torsional moment spectra determined by the proposed formulas match with those by the wind tunnel test well, indicating that the proposed formulas provide reasonable predictions for the power spectra of the wind-induced torques on L-shaped tall buildings.

### 3.4.2. The RMS torque coefficients

Taking the relative height $z/H$ as a parameter, the polynomial expression shown in Eq. (17) is used to fit the RMS torque coefficients of the L-shaped building models, in which $t_1', t_2'$ and $t_3'$ are parameters involved in Eq.(17). The NLSM is then adopted to fit the parameters in terms of the side ratio and the terrain category.

$$C_T'(z) = t_1' + t_2'\left(\frac{z}{H}\right) + t_3'\left(\frac{z}{H}\right)^2 \tag{17}$$

$$t_1' = 0.0026 + 0.0017\alpha_{TR} + (0.0482 - 0.0042\alpha_{TR})\alpha_{DB} - (0.0007 + 0.0015\alpha_{TR})\alpha_{DB}^{2} \tag{18}$$

$$t_2' = 0.1202 + 0.0238\alpha_{TR} - (0.0369 + 0.0213\alpha_{TR})\alpha_{DB} + (0.0049 + 0.0061\alpha_{TR})\alpha_{DB}^{2} \tag{19}$$

$$t_3' = -0.0028 - 0.0094\alpha_{TR} - (0.0257 + 0.0105\alpha_{TR})\alpha_{DB} - (0.0068 + 0.0018\alpha_{TR})\alpha_{DB}^{2} \tag{20}$$

In order to validate the above empirical formulas, errors between the experimental results and those calculated by the formulas are illustrated in Fig. 11. The error rate is defined in Eq. (20). It can be found that the error rates of all the parameters are smaller than 5%, thus verifying the applicability of the proposed formulas.

$$ER = \frac{Estimated\ \ Value - Test\ \ Value}{Test\ \ Value} \times 100\% \tag{20}$$

### 3.4.3. Vertical correlation coefficients

Correlation coefficient represents mutual dependence of two random variables. Vertical correlation coefficient $Cor_F(z_i, z_j)$ is defined

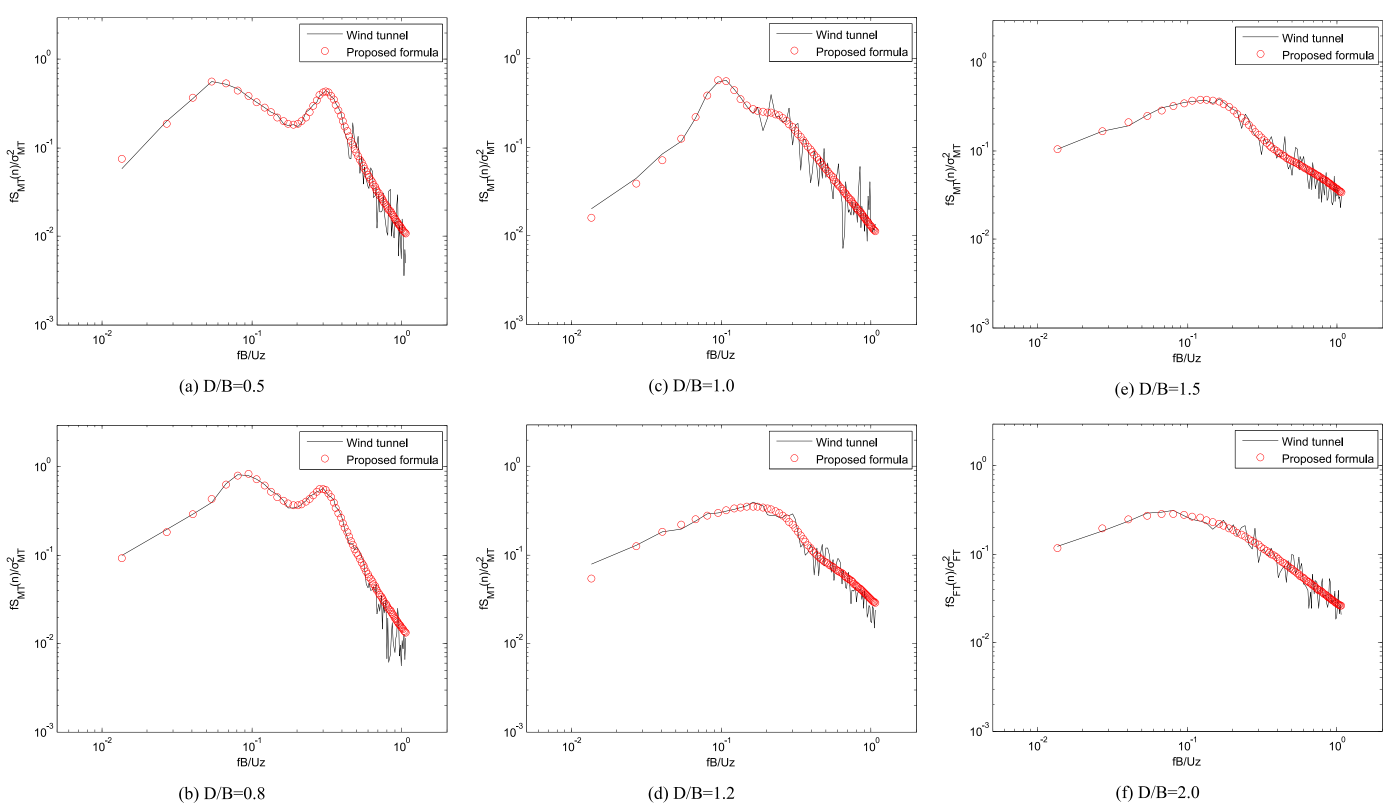


**Fig. 10.** Comparisons of base torque spectra by the proposed formulas and the test results.

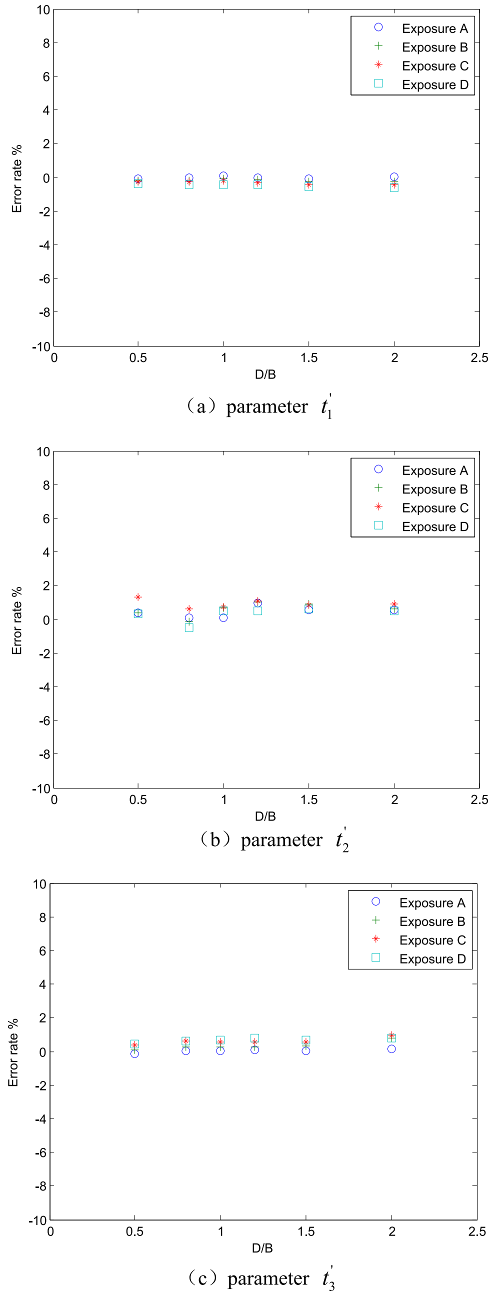


**Fig. 11.** Errors between the test results and those calculated by the proposed formulas.

below.

$$Cor_F(z_i, z_j) = \frac{Cov_F(z_i, z_j)}{\sigma_F(z_i)\sigma_F(z_j)} \tag{21}$$

where $Cov_F(z_i, z_j)$ is the covariance of torque coefficients between heights $z_i$ and $z_j$.

As shown in Fig. 12, the vertical correlation coefficients almost range from 0.1 to 0.7. When $D/B < 1$, the vertical correlation coefficients rapidly decrease as the relative height increases and the results seem to be scattered. When $D/B \geq 1$, the vertical correlation coefficients gradually decrease as the side ratio increases. Vickery and Clark (1972) indicated that the wake excitation contributed a lot in wind-induced torques and wind-induced responses of stacks. They proposed an exponential function for the wake excitation. However, the parameters in the proposed function are available only for some fixed side ratios of tapered stacks. Based on the wind tunnel test results of this study, a new expression of the vertical correlation coefficients is established as a function of the side ratio and the terrain category as follows.

$$Cor_F(z_i, z_j) = \beta_T \times \exp(-\eta_T x) \quad x = |z_i - z_j|/H \tag{22}$$

where, $x = |z_i - z_j|/H$; $\beta_T$, $\eta_T$ are parameters varied with the side ratio and the terrain category, and they are expressed as follows.

$$\beta_T = 0.7312 + 0.0547\alpha_{TR} + (0.0508 - 0.0088\alpha_{TR})\ln(\alpha_{BD}) - (0.0043 + 0.0121\alpha_{TR})\alpha_{BD}^{-2} \tag{23}$$

$$\eta_T = 0.8450 + 0.0054\alpha_{TR} + (0.0857 - 0.0129\alpha_{TR})\alpha_{BD}^{2} + (1.8148 - 0.1202\alpha_{TR})\alpha_{BD}^{-1} \tag{24}$$

Curves in Fig. 12 show the fitted results for terrain category C. The vertical correlation coefficients calculated by the expression keep good consistent with the test results, although there are some discrepancies between the predictions and the measurements. In general, the proposed formula can effectively describe the variations of the vertical correlation coefficients with the side ratio and the terrain category.

In the light of the theory of random vibration, the *kth* generalized force spectrum can be expressed as

$$S_{Fk}^*(f) = \int_0^H \int_0^H S_F(z_i, z_j; f)\varphi_k(z_i)\varphi_k(z_j)dz_i dz_j \tag{25}$$

where, $\varphi_k(z_i)$,$\varphi_k(z_j)$ are the *kth* mode shape at heights of $z_i$ and $z_j$. When substituting Eq. (3) into Eq. (25) and combining Eq. (1), the *kth* generalized force spectrum is simplified as follows:

$$S_{Fk}^*(f) = \frac{(0.5\rho U_H^2)^2 A(z_i)A(z_j)D^2 S_{M_T}(f)}{\sigma_{M_T}^2} \times \int_0^H \int_0^H C_T'(z_i)C_T'(z_j) Cor_F(z_i, z_j)\varphi_k(z_i)\varphi_k(z_j)dz_i dz_j \tag{26}$$

## 4. Case study

A practical project is chosen as a case study to validate the proposed formulas for evaluating the wind-induced torques on L-shaped tall buildings. The practical project involved the wind-resistant design of a nearly L-shaped tall building made of reinforced concrete. The damping ratio is supposed to be 5% according to the specification of the local design code (JGJ 3-2010, 2010). The height of the building is 333 m and the cross section dimension B×D is 47.5 m×71.1 m. Terrain category C is chosen for the wind-resistant design of the tall building according to the situation of surrounding buildings. The first-order torsional frequency determined from the structural dynamics analysis of the building is 0.231 Hz. Wind tunnel test of the building model with geometric scale of 1:500, as shown in Fig. 13, was conducted to determine the wind loads and wind-induced response of the tall building. The reference mean wind speed at the top of the building model was 10 m/s during the wind tunnel test. Fig. 14 shows the definition of wind direction and plan section of the building model.

It was found through the model test that 270° is the unfavorable wind direction for the wind-induced torques on the building model. Comparison of the generalized base torsional moment spectrum determined by the proposed formula and the experimental measurements is shown in Fig. 15. Since the side ratio is 1.497, the measured generalized base torque spectrum is very gentle as the reduced frequency increases. Although the shape of this building does not exactly match the L-shape geometry, its side ratio, terrain category of the building site and the unfavorable wind direction are consistent with those considered in the study. It is evident that the spectrum fitted by the proposed formula agree with the test results well, indicating the simplified expression proposed in this paper can reasonably predict the wind-induced torques on L-shaped tall buildings.

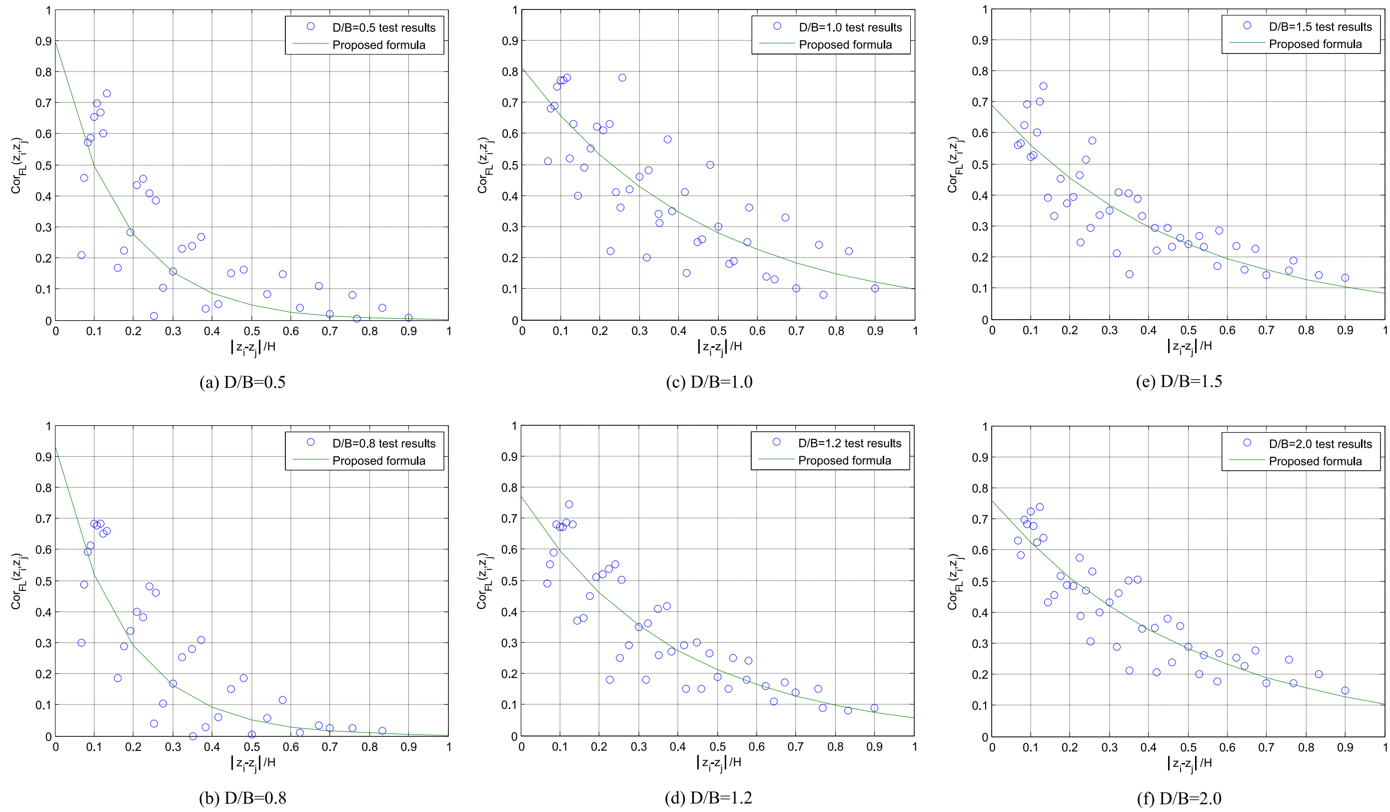


**Fig. 12.** Comparisons of vertical correlation coefficients by the proposed formula and the test results.

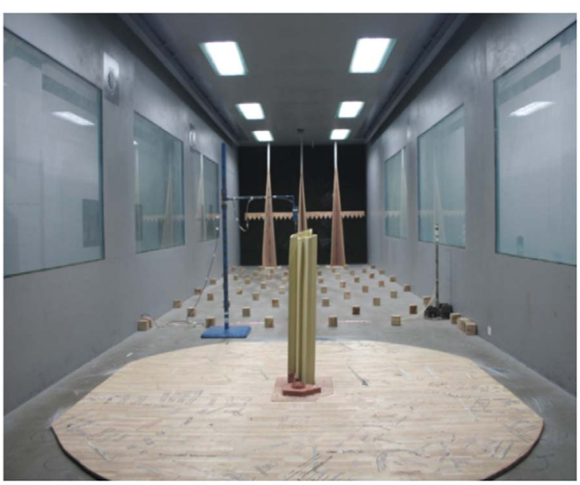

**Fig. 13.** Model in wind tunnel test.

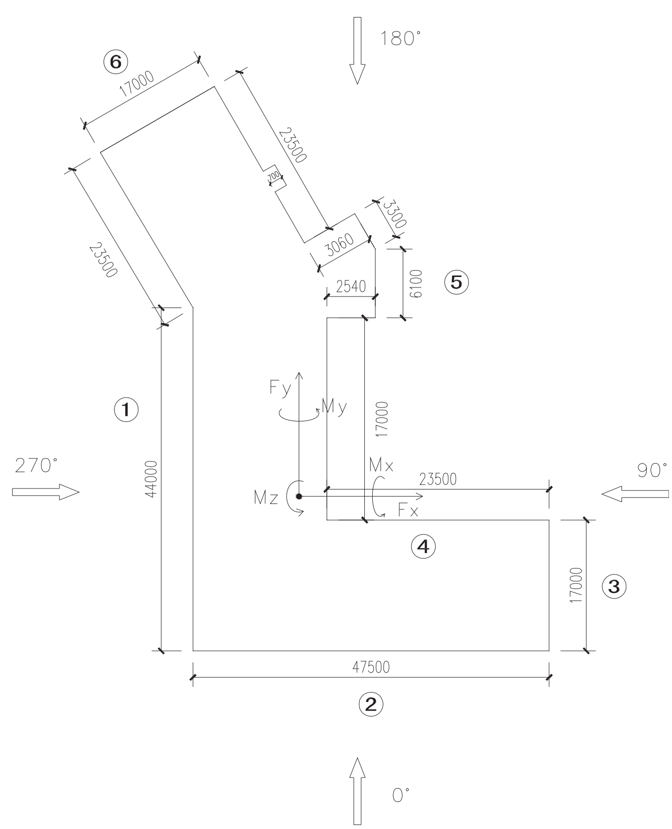


**Fig. 14.** Definition of wind direction and plan section view.

## 5. Conclusions

Based on extensive wind tunnel test results, this paper investigated the characteristics of wind-induced torques on L-shaped tall buildings. The RMS force coefficients, power spectral densities and vertical correlation functions of the wind-induced torques were presented and discussed. The main conclusions of this study are summarized as follow:

(1) The terrain category has little effect on the mean torque coefficients in all wind directions. The RMS torque coefficients gradually increase as the level of turbulence intensity of approaching wind flow increases.
(2) The mean torque coefficients gradually increase as the side ratio increases. The maximum value of the mean torque coefficients arrive at 0.28 and cannot be ignored in the wind-resistant design. The RMS torque coefficients change little as the height of L-shaped buildings increases but slightly increase as the side ratio increases.

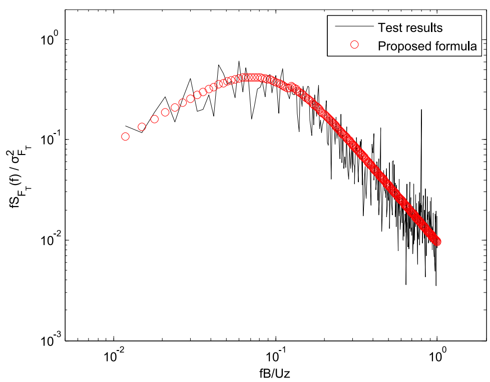


**Fig. 15.** Comparison of the generalized base torque spectra.

The effects of the aspect ratio are insignificant.

(3) The mean and RMS base torsional moment coefficients varying with approaching wind direction are in consistent patterns with those of the torque coefficients. The mean base torsional moment coefficients range from −0.14 to 0.28 and the RMS base torsional moment coefficients vary from 0.009 to 0.065 in all wind directions.

(4) The variations of the base torsional moment spectra with the reduced frequency are almost the same as those of the torque spectra at each measurement layer on L-shaped building models. When $D/B < 1$, there are two peaks emerged in the torque spectra due to vortex shedding and reattachment of separated flow on the side wall. When $D/B = 1$, there is only a narrow-band peak emerged in the torque spectra and the reduced frequency corresponding to the peak is close to the Strouhal number (0.1) of rectangular cylinders. As the side ratio $D/B$ continues to increase, the torque spectrum becomes similar with longitudinal velocity spectrum and changes slightly as the frequency increases.

(5) When $D/B < 1$, the vertical correlation coefficients rapidly decrease as the relative height increases and the results seem to be scattered. When $D/B \geq 1$, the vertical correlation coefficients gradually decrease as the side ratio increases. The vertical correlation coefficients range from 0.1 to 0.7.

(6) Empirical formulas of base torsional moment spectra, RMS torque coefficients and vertical correlation coefficients of L-shaped tall buildings were proposed by taking the side ratio and the terrain category as two basic variables. A case study verified the applicability of the proposed formulas for evaluating the wind-induced torques on L-shaped tall buildings.

## Acknowledgments

The work described in this paper was fully supported by the grants from National Nature Science Foundation of China (Project no: 51478405, 51408062) and a grant from the Research Grants Council of Hong Kong Special Administrative Region, China (Project No: CityU 11256416). The authors would like to thank the support from Hubei Key Laboratory of Roadway Bridge and Structure Engineering at Wuhan University of Technology (Project no: DQJJ201502).

## References

AIJ Recommendations for Loads on Buildings, 2004Architectural Institute of Japan, Tokyo, Japan.
ASCE: 7-10, 2010. Minimum Design Loads for Buildings and other Structures. Structural Engineering Institute of the American Society of Civil Engineering, Reston.
Chakraborty, S., Dalui, S.K., Ahuja, A.K., 2014. Wind load on irregular plan shaped tall building-a case study. Wind Struct. 19 (1), 59–73.
Cheng, L., Lam, K.M., Wong, S.Y., 2015. POD analysis of crosswind forces on a tall building with square and H-shaped cross sections. Wind Struct. 21 (1), 63–84.
Cluni, H., Gusella, V., Spence, S.M.J., Bartoli, G., 2011. Wind action on regular and irregular tall buildings: high order moment statistical analysis by HFFB and SMPSS measurements. J. Wind Eng. Ind. Aerod. 99, 682–690.
GB50009-2012, 2012. Load Code for the Design of Building Structures. China Architecture & Building Press, Beijing.
Gomes, M., Rodrigues, A., Mendes, P., 2005. Experimental and numerical study of wind pressure on irregular-plan shapes. J. Wind Eng. Ind. Aerod. 93 (10), 741–756.
Gu, M., 2009. Study on wind loads and response on tall buildings and structures, In: Proceedings of the Seventh Asia Pacific Conference, Taipei, Taiwan.
JGJ 3-2010, 2010. Technical Specification for Concrete Structures of Tall Building. China Architecture & Building Press, Beijing.
Kim, Y.C., Kanda, J., 2013. Wind pressures on tapered and set-back tall buildings. J. Fluids Struct. 39, 306–321.
Li, Y., 2014. Research on Wind Load Characteristics and Optimal Design of Tall Buildings with Irregular Plane (Ph.D. Dissertation). Hunan University, Changsha.
Li, Y., Li, Q.S., 2016. Across-wind dynamic loads on L-shaped tall buildings. Wind Struct. 23 (5), 385–403.
Li, Y., Zhang, J.W., Li, Q.S., 2014. Experimental investigation of characteristics of torsional wind loads on rectangular tall buildings. Struct. Eng. Mech. 49 (1), 129–145.
Liang, S.G., Li, Q.S., Liu, S.C., Zhang, L.L., Gu, M., 2004. Torsional dynamic wind loads on rectangular tall buildings. Eng. Struct. 26 (1), 129–137.
Lin, N., Letchford, C., Tamura, Y., Liang, B., Nakamura, O., 2005. Characteristics of wind forces acting on tall buildings. J. Wind Eng. Ind. Aerod. 93 (3), 217–242.
Stathopoulos, T., Zhou, Y., 1993. Numerical simulation of wind induced pressures on buildings of various geometries. J. Wind Eng. Ind. Aerod. 46/47, 419–430.
Tallin, A., Ellingwood, B., 1984. Serviceability limit states: wind induced vibrations. J. Struct. Eng., ASCE 110 (10), 2424–2437.
Tallin, A., Ellingwood, B., 1985. Analysis of torsional moments on tall buildings. J. Wind Eng. Ind. Aerod 18 (2), 191–195.
Tang, Y., 2006. Research on the wind excited vibrations and static-equivalent wind loads of torsionally coupled high-rise buildings (Ph.D. Dissertation). Tongji University, Shanghai.
Vickery, B.J., Clark, A.W., 1972. Lift or Across-wind Response of Tapered StacksJ. Struct. Div. ASCE ST1, 1–20.